Slow dynamics of nanocomposite polymer aerogels as revealed by X-ray photocorrelation spectroscopy (XPCS)

Rebeca Hernández, Aurora Nogales, Michael Sprung, Carmen Mijangos, and Tiberio A. Ezquerra

Citation: The Journal of Chemical Physics **140**, 024909 (2014); doi: 10.1063/1.4861043
View online: http://dx.doi.org/10.1063/1.4861043
View Table of Contents: http://scitation.aip.org/content/aip/journal/jcp/140/2?ver=pdfcov
Published by the AIP Publishing

Slow dynamics of nanocomposite polymer aerogels as revealed by X-ray photocorrelation spectroscopy (XPCS)

Rebeca Hernández,[1,a)] Aurora Nogales,[2,a)] Michael Sprung,[3] Carmen Mijangos,[1] and Tiberio A. Ezquerra[2]
[1]*Instituto de Ciencia y Tecnología de Polímeros, ICTP-CSIC, Juan de la Cierva, 3, 28006 Madrid, Spain*
[2]*Instituto de Estructura de la Materia, IEM-CSIC, Serrano 121, 28006 Madrid, Spain*
[3]*Petra III at DESY, Notkestr. 85, 22607 Hamburg, Germany*

(Received 20 September 2013; accepted 19 December 2013; published online 13 January 2014)

We report on a novel slow dynamics of polymer xerogels, aerogels, and nanocomposite aerogels with iron oxide nanoparticles, as revealed by X-ray photon correlation spectroscopy. The polymer aerogel and its nanocomposite aerogels, which are porous in nature, exhibit hyper-diffusive dynamics at room temperature. In contrast, non-porous polymer xerogels exhibit an absence of this peculiar dynamics. This slow dynamical process has been assigned to a relaxation of the characteristic porous structure of these materials and not to the presence of nanoparticles. © *2014 AIP Publishing LLC*. [http://dx.doi.org/10.1063/1.4861043]

I. INTRODUCTION

A polymer gel can be defined as a crosslinked polymeric or copolymeric network which is characterized by a remarkable ability to absorb a considerable quantity of liquid up to swelling equilibrium without being dissolved. When the swollen liquid is water, the polymer gel is called hydrogel.[1] Due to their crosslinked structure, porous polymer materials can be obtained by drying polymer hydrogels.[2,3] Porous polymer materials have attracted a lot of attention due to their applications mainly in biomedicine as scaffolds for tissue engineering[4] or drug delivery matrices.[5] In this regards, it is very important to control the drying conditions in order to preserve the network structure. Standard evaporation of the solvent from the hydrogel results in a dry gel, referred to as "xerogel," for which a strong collapse of the initial structure has been observed.[6] On the contrary, hydrogels dried under supercritical conditions retain most of the volume of the pristine hydrogel and present high surface areas. The gel does not shrink, so the fragile network is unchanged and the resulting material is highly porous.[7] These dry gels are designated as "aerogels." Polymer hydrogels dried by freeze-drying give rise to materials that were initially known as cryogels, more recently also termed aerogels.[6] Freeze drying consists of lowering the temperature of the solvent below the crystallization temperature. The solvent is then removed as a vapor by reducing the pressure (sublimation).

Literature regarding the investigation of dynamics of porous polymeric materials is very scarce. Some papers can be found regarding the determination of dynamics exhibited by aerogels.[8–10] These materials present an hyperdifussive dynamics, characterized by compressed exponential correlation functions with a characteristic relaxation time, τ, that varies inversely with the modulus[11] of the scattering vector q as $\tau \sim q^{-1}$. The dynamics encountered for these materials were attributed to a characteristic length related to the typical molecular size.[10] Interestingly enough, a great variety of soft materials such as polymer nanocomposites,[12,13] block-copolymer phases,[14] colloidal glasses,[15,16] gels[17,18] or polymer thin-film surfaces and interfaces[19] share in common hyper-diffusive motion, which seems to be a common feature of jammed systems.

An additional interest in the determination of the dynamics of aerogels appears when nanoparticles are added to obtain nanocomposite (NC) aerogels. In fact, the incorporation of nanoparticles or nanofibers into aerogels gives rise to materials strong enough to withstand mechanical stress of repeated use with only a small effect on density or porosity. These NC aerogels may be employed in advanced applications which demand lighter-weight, robust, dual purpose materials for energy applications,[20] water disinfection[21] or biomedical applications.[22]

In spite of the vast literature regarding polymer nanocomposites,[23–28] there are no studies aimed to determine the slow dynamics present in nanocomposite aerogels consisting of highly porous crosslinked polymer matrixes in which nanoparticles are incorporated. In this paper, we present for the first time an X-ray photon correlation spectroscopy (XPCS) investigation aimed at determining the dynamics of NC aerogels, obtained through freezing-drying of semi-interpenetrating polymer networks of alginate (Alg) and poly(N-isopropylacrylamide) (PNiPAAm) with iron oxide nanoparticles. In addition, we compare the results to those obtained for samples without nanoparticles, aerogels, and xerogels dried at room temperature.

II. EXPERIMENTAL

A. Sample preparation

Samples were prepared as reported in Ref. 29, briefly, semi-interpenetrating polymer hydrogels (semi-IPHs) of alginate/poly(N-isopropylacrylamide) (Alg-PNiPAAm)

a)Authors to whom correspondence should be addressed. Electronic addresses: rhernandez@ictp.csic.es and aurora.nogales@csic.es.

TABLE I. Samples under study.

Sample name	Drying method	%Wt. iron oxide[a]
Alg-PNiPAAm (X)	Evaporation of water	0
Alg-PNiPAAm (A)	Freeze-drying	0
FeAlg-PNiPAAm (10)	Freeze-drying	10
FeAlg-PNiPAAm (18)	Freeze-drying	18

[a]Determined through thermogravimetric analysis.

where obtained through radical copolymerization of N-isopropylacrylamide (N-AAm) and N,N´-methylene bisacrylamide (BIS) (molBIS/mol N-AAm = 3%) in the presence of a 1 wt.% alginate aqueous solution. *In situ* synthesis of iron oxide nanoparticles inside Alg-PNiPAAm semi-IPHs was carried out by coprecipitation of iron cations in basic solution. The concentration of iron oxide nanoparticles was varied by repeating the coprecipitation step, in this way we were able to obtain swollen Alg-PNiPAAm semi-IPHs with different iron oxide contents. Thermogravimetric measurements were performed on dried gels on a Q500 TA Instruments TGA, using a nitrogen stream as the purge gas, at a heating rate of 10 °C/min over the range 40–900 °C. Considering that the Alg-PNiPAAm semi-IPH decomposes completely at 900 °C, the residual weight obtained for the samples with iron oxide can be taken as an indication of the iron oxide content in the samples.[29] Samples were designated as FeAlgPNiPAAm (10) and FeAlgPNiPAAm (18) where the numbers in brackets denote the iron oxide content, 10 wt.% and 18 wt.%, respectively, as determined through TGA measurements.

Diameters corresponding to primary particles and aggregates formed by primary particles were determined from model fits to ultra-small angle X-ray scattering as previously reported.[30] The size of the individual nanoparticles was ∼20 nm for FeAlgPNiPAAm (10) and FeAlgPNiPAAm (18). Both samples presented the same degree of dispersion of the individual nanoparticles with an aggregate size of ∼100 nm.

For the XPCS experiments reported in this paper, swollen Alg-PNiPAAm hydrogels were dried in two different ways. On the one hand, xerogels (X) were obtained by slowly evaporating the solvent at ambient temperature and atmospheric pressure. On the other hand aerogels (A) were obtained through a process of freeze-drying. Samples containing nanoparticles, FeAlg-PNiPAAm (10) and FeAlg-PNiPAAm (18) were both freeze-dried to yield nanocomposite aerogels.

Table I describes the sample names chosen for all the samples under study.

B. Scanning electron microscopy (SEM)

All the samples under study were fractured and coated with gold, the surface morphology was studied in a Philips XL-30 ESEM. Pore size distribution was analyzed using the public domain NIH Image program (http://rsb.info.nih.gov/nih-image).

C. X-ray photocorrelation spectroscopy

XPCS experiments were performed at the beam line P10 of PETRA III using 7 keV x-rays. A pixelated 2D detector (Princeton Instruments PI-LCX), located at 5.08 m downstream of the sample, was used to record the scattering patterns. The detector consists of 1340 × 1300 pixels each having an area of 20 × 20 μm^2. A q range from 0.012 to 0.0647 nm^{-1} was covered. In order to avoid radiation damage of the sample, for every measurement 500 frames with an acquisition time of 0.1 s and a delay time (waiting time between two consecutive frames) of 2.5 s were recorded.

Experimentally, we measure the normalized intensity-intensity autocorrelation function $g^{(2)}$ (q, t), which is related to the intermediate scattering function (ISF, f (q, t)) as

$$g^{(2)}(q,t) = 1 + b[f(q,t)]^2, \quad (1)$$

where b and t are the instrument dependent Siegert factor and the delay time, respectively.[31,32]

In order to check for aging phenomena, non-stationary dynamics as a function of time, the correlation analysis was explicitly performed as a function of aging time, by considering different time intervals starting from the beginning of the experiment (t = 0) each at a fixed q-value.

All measurements were carried out at T = 25 °C and each experiment was repeated several times to ensure reproducibility.

III. RESULTS AND DISCUSSION

Representative images obtained by scanning electron microscopy corresponding to Alg-PNiPAAm (X), AlgP-NiPAAm(A), and FeAlgPNiPAAm (10) are shown in Figure 1. The morphology of Alg-PNiPAAm (X) consists of a continuous film with no appreciable porosity at the investigated length scale. In contrast, the morphology of the aerogels consists of an interconnected pore structure. The histograms corresponding to the pore size distribution of samples Alg-PNiPAAm (A) and FeAlg-PNiPAAm (10) calculated from the analysis of the SEM images are shown in the insets of Figures 1(b) and 1(c), respectively. Both samples show similar distribution of pore sizes centered at a pore size of ∼5 μm.

Figure 2 shows the intensity autocorrelation functions measured at room temperature by means of XPCS for the aerogel sample with no iron oxide nanoparticles (NPs). Here, a series of simultaneously measured curves for different values of q is shown.

The experiments clearly reveal the existence of a dynamic process at T = 25 °C in the time scale investigated by XPCS. It is also clear that the dynamics becomes slower as the value of q decreases. Numerous studies[31,33,34] have reported that the ISF, and consequently $g^{(2)}$ (q, t) are best described by means of a Kohlrausch-Williams-Watts (KWW) expression:

$$g^{(2)}(q,t) = B + A\exp\left(-2\left[\frac{t}{\tau(q)}\right]^{\beta(q)}\right), \quad (2)$$

where β is the Kohlrausch exponent denoting the deviation from a single Debye relaxation ($\beta = 1$) and τ is the relaxation

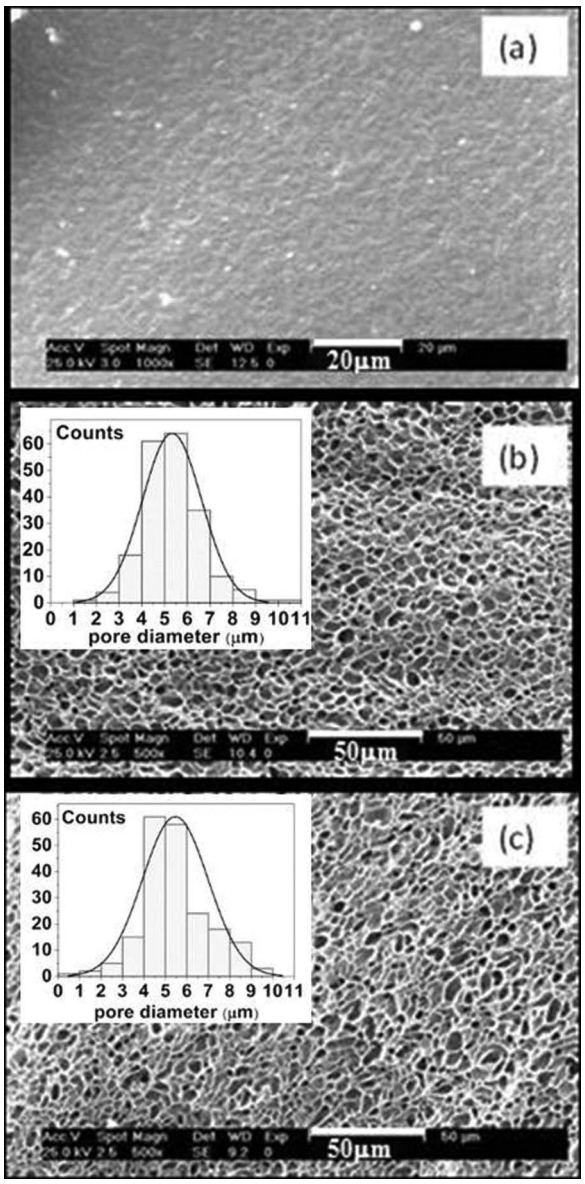

FIG. 1. Scanning electron microscopy corresponding to (a) Alg-PNiPAAm (X), (b) Alg-PNiPAAm (A), and (c) FeAlg-PNiPAAm (10). Insets in Figs. 1(b) and 1(c) show pore size distribution (gray bars) determined from analysis of the corresponding SEM images and fitting to a log-normal distribution (solid black line).

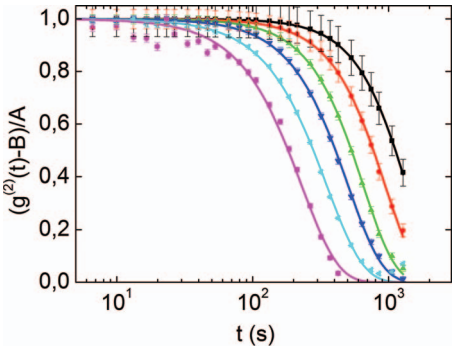

FIG. 2. XPCS intensity autocorrelation functions taken at room temperature for different values of q for the sample Alg-PNiPAAm (A). (black ■) q = 0.012 nm^{-1}, (red ●) q = 0.016 nm^{-1}, (green ▲) q = 0.0217 nm^{-1}, (navy ▼) q = 0.0294 nm^{-1}, (blue ◄) q = 0.0397 nm^{-1}, and (magenta ●) q = 0.0532 nm^{-1}. Continuous lines are fits to Eq. (2).

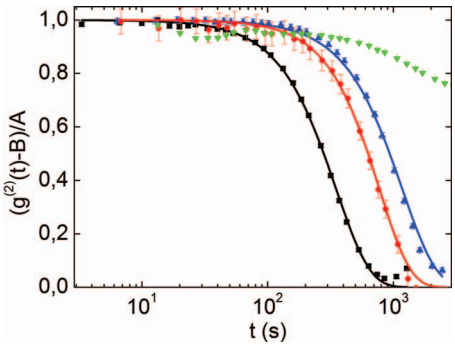

FIG. 3. (a) XPCS intensity autocorrelation functions taken at q = 0.0412 nm^{-1} for the samples under study: (green ▼) Alg-PNiPAAm (X), (black ■) Alg-PNiPAAm (A), (red ●) FeAlgPNiPAAm (10), and (blue ▲) FeAlgPNiPAAm (18). Continuous lines are fits to Eq. (2).

time of the process, B is the baseline and A is associated to the contrast. The data in Figure 2 can be well described by Eq. (2) assuming KWW exponents values $\beta > 1$, which indicate a strong non-exponential character of the relaxation. Fig. 3 shows the intensity autocorrelation functions measured at T = 25 °C at a fixed q = 0.0412 nm^{-1} for all the samples under study.

An important result that can be extracted from Figure 3 is the absence of significant observable dynamics of the sample Alg-PNiPAAm (X) in comparison to those of the aerogels obtained through freezing-drying. In addition, for aerogels, a slowdown of the dynamics in the nanocomposite aerogels is observed with respect to the sample with no nanoparticles (Alg-PNiPAAm (A)). In these cases, a good description of the XPCS data can also be obtained by using Eq. (1) with $\beta > 1$ as indicated by the continuous lines shown in Figure 3.

In order to check whether dynamics were stationary during the time of experiment, the correlation analysis was explicitly performed up to different time intervals starting from the beginning of the experiment (t = 0) each at a fixed q-value. Figure 4 displays XPCS intensity autocorrelation functions at q = 0.0412 nm^{-1} for samples AlgPNiPAAm (A) and FeAlgPNiPAAm (18) measured at four different times since the beginning of the XPCS experiment. From these plots, it is not possible to draw conclusions on possible changes of the characteristic relaxation times obtained at different times of the experiment because a complete decay of the correlation functions is not achieved at short times of experiment, more remarkably for sample FeAlgPNiPAAm (18).

Further information can be retrieved from two-time correlation function G (q, *t*1, *t*2):[10,35,36]

$$G(q,t1,t2) = \frac{\langle I(q,t1)I(q,t2)\rangle_{pix}}{\langle I(q,t1)\rangle_{pix}\langle I(q,t2)\rangle_{pix}}. \quad (3)$$

Here, the ensemble averages are performed over many pixels of the CCD detector, all having the same q value. The variables to describe the two-time correlation function are the average time or age $t_a = (t_1 + t_2)/2$, measured by the distance along the $t_1 = t_2$ diagonal in the perpendicular direction and the time difference $t = t_1 - t_2$, which is the distance from the $t_1 = t_2$ diagonal in the perpendicular direction. In an equilibrium system, the two time correlation functions depend only

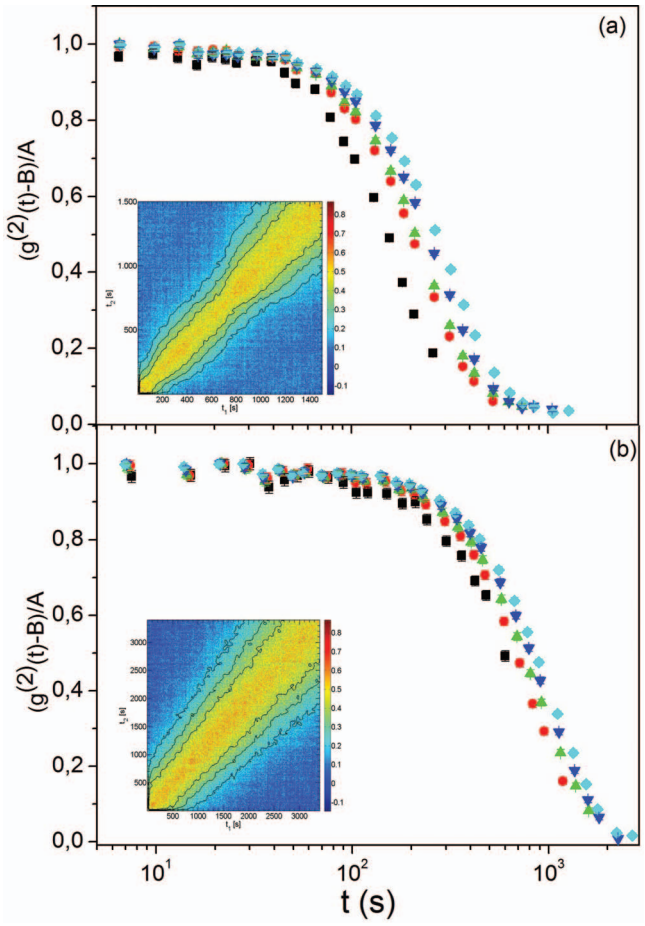

FIG. 4. XPCS intensity autocorrelation function at q = 0.0412 nm^{-1} for (a) Alg-PNiPAAm (A) obtained up to : (black ■) 260 s, (red ●) 525 s, (green ▲) 736 s, (navy ▼) 1050 s, and (blue ♦) 1280 s and (b) FeAlgPNiPAAm (18): (black ■) 601 s, (red ●) 1180 s, (green ▲) 1610 s, (navy ▼) 2270 s, and (blue ♦) 2670 s. Insets show the two-time correlation function G (q = 0.0412 nm^{-1}, t_1, t_2) obtained for each of the samples.

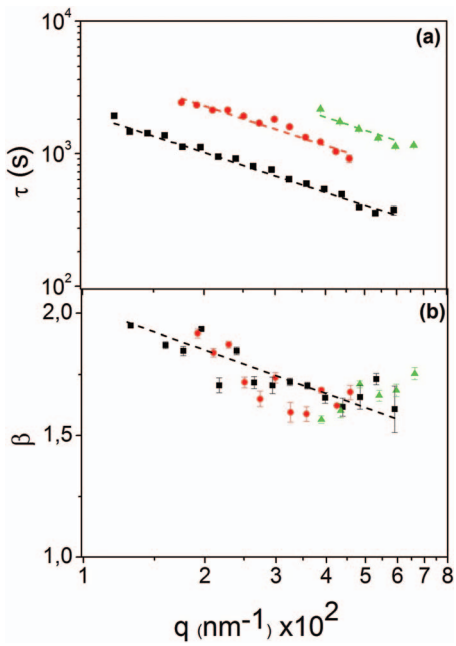

FIG. 5. (a) Relaxation time, τ, plotted against q on a log-log scale (dashed lines are linear fits) and (b) compressed exponent β vs. q for the three samples under study (dashed line is a guide to the eye): (black ■) Alg-PNiPAAm (A), (red ●) FeAlgPNiPAAm (10), and (green ▲) FeAlgPNiPAAm (18).

on the time difference t, and hence the two time correlation contour lines are parallel.

The iso-intensity lines in plots G (q, *t*1, *t*2) (insets Figure 4) corresponding to both samples show a slight increase in the width perpendicular to the diagonal which indicates slowing-down of dynamics with time. Even if samples were prepared well before the X-ray measurements, so that an equilibrium state can be expected, a possible explanation for the non-stationary dynamics observed is the internal stress in the structure induced by the simple manipulation of the sample that results in "aging" of the samples.[10]

The q-dependence of τ extracted from the fittings of $g^{(2)}$ (q, t) (Eq. (2)) to our data for the aerogel samples under study is shown in Figure 5(a) in double logarithmic scale.

For the two nanocomposite samples, only parameters extracted from experiments carried out at q values higher than 0.025 nm^{-1} were considered since, for these q values, the dynamics decay to 1/e of its initial value. For the three cases it is evident that, independently of the presence of nanoparticles, a power law dependence of τ with q is found.

Dotted lines in Fig. 5(a) indicate the fits to a power-law form of the type $\tau \sim q^{-1}$ in the experimental data accessible in the q-range under study. This dependence is also indicative of a ballistic dynamics as explained above. A representation of the parameter β as a function of q extracted from the fitting to Eq. (2) is shown in Figure 5(b). The samples tend to present a similar q-dependence of β with values decreasing from 2 to 1.5 as q increases. It is clear that the slow relaxation behavior observed here for both the aerogel and its nanocomposites present an hyper-diffusive behavior resembling very much that encountered for colloidal suspensions.[15,16,37] Specifically, there are two leading hypotheses for the origin of the hyperdiffusive dynamics: (i) long-wavelength strain motion and (ii) continuous-time random walk (CTRW) behavior.[10] CTRW behavior has been proposed in the context of hyperdiffusive nanoparticle motion in solutions.[37] Subdiffusive behaviour has been reported for gold nanoparticles motion in polymer nanocomposites[34] where the nanoparticles are passive tracers of the intrinsic polymer motion.

The first question to be answered would be related to the origin of the dynamics in our experiments. One possibility would be that the dynamics could be associated to the polymer matrix. XPCS experiments were carried out at T = 25 °C and thus well below the glass transition of the samples under investigation being T_g = 155 °C for Alg-PNiPAAm (A) and slightly increasing with the iron oxide NPs content up to a Tg = 157 °C for the sample FeAlg-PNiPAAm (10). Therefore, it is unlikely that the slow dynamics observed can be considered as intrinsic to the polymer matrix. This is reinforced by the fact that the aerogel (Alg-PNiPAAm (A)) presents dynamics in the q-range under investigation whereas the xerogel (Alg-PNiPAAm (X)) does not, even if both samples have a T_g well above room temperature derived from the PNiPAAm crosslinked structure independently of the process of

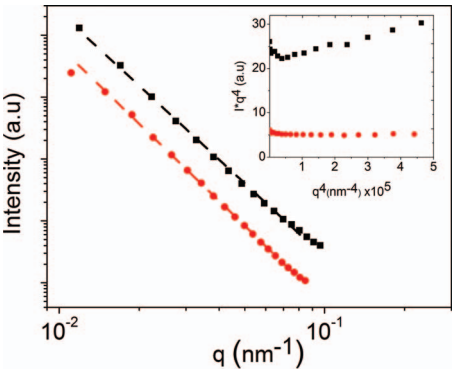

FIG. 6. Double logarithmic plot of the scattered SAXS intensity as a function of q for (black ■) Alg-PNiPAAm (X) and (red ●) Alg-PNiPAAm (A). Dashed lines represent linear fitting to the experimental data. The inset shows a representation of I (q)*q^4 with respect to q^4 for both samples under study.

drying. Further conclusions on the origin of the dynamics observed can be obtained from the analysis of the Small Angle X-ray Scattering (SAXS) of Alg-PNiPAAm (X) and Alg-PNiPAAm (A) samples. The scattering patterns from samples studied here are completely isotropic. A representation of the azimuthally averaged SAXS intensities I (q) as a function of q is shown in Figure 6.

In both cases the most prominent feature is a linear decrease of the intensity in a log-log scale with a slope of −4 which is characteristic of a Porod regime.[38] The dotted lines represent the fit of the data to a $I\alpha K/q^4$ scaling law for the scattered intensity. This behavior can be attributed to the scattering of the sharp interfaces of scattering elements. In particular, Porod law behavior for the SAXS scattered intensity has been previously reported in a series of silica aerogels and has been discussed as due to the pore interfaces.[39]

In our case, although similar at first glance, a representation of data on a Porod Plot (I*q^4 versus q^4) evidences differences between both samples (inset Figure 6). Here one sees that the sample Alg-PNiPAAm (A), with a well-defined pore structure as revealed by the SEM images (Fig. 1(b)), exhibits the characteristic feature of a Porod behavior, in this case an independency of I*q^4 with q^4. The Alg-PNiPAAm (X) sample, with no pores as revealed by the SEM images (Fig. 1(a)), exhibits a behavior of the type $I\alpha I_b + K/q^4$ where I_b is referred to as the liquid scattering appearing form local electron density fluctuations.[40] Accordingly, in the q-range investigated we can infer that the scattering of the Alg-PNiPAAm (A) is dominated by the interfaces formed by the pore walls of the sample. Given the absence of observable dynamics in the sample with no pores (Alg-PNiPAAm (X)), we propose to assign the relaxation process to a slow dynamics corresponding to internal motion of pores of the aerogels, that is, fluctuating pore walls. Therefore, the electron density difference between the pores and the polymer walls of the sample can be pointed as the origin of the main scattered intensity. In samples with nanoparticles, FeAlg-PNiPAAm (10) and FeAlg-PNiPAAm (18), an important contribution from the scattering of the nanoparticles is obtained in the q-range under study as previously reported[30] which might overlap with the contribution to the scattering of the interfaces. Following from this, since both polymer aerogel and its nanocomposite aerogels exhibit qualitatively similar XPCS signals, the nanoparticles motions independent from that of the polymer matrix can be ruled out as the origin of the observed sample dynamics. In the case of nanoparticles suspended in a supercooled glass forming liquid, ballistic dynamics is observed when the temperature is lowered reflecting the onset of dynamical heterogeneity.[37] Correlation functions with $\beta = 1.5$ and $\tau \sim q^{-1}$ can be associated with relaxation of heterogeneous local stress in the limit where the sources of internal stress are diluted and the strain intensities are predominantly dipolar.[41] This behavior has been previously observed in mechanically reinforced polymer nanocomposites because of their gel-like properties,[23] together with a number of other soft systems such as colloidal gels of particles with attractive interactions, pastes and foams due to the emergence of elasticity.[16] In our case, pores in aerogels and NC aerogels exhibit a slow relaxation which seems to mimic that of particle colloidal suspensions,[37] the pore being equivalent to a soft particle subjected to severe jamming conditions exerted by the polymer walls. However, considering that the average pore size is of about 5 μm (see histograms shown in Figure 1), it is not likely that the motion of the pores as a whole is the origin of the observed dynamics. This interpretation is reinforced by the fact that the length scales proven in the accessible q-range in the static SAXS measurements (0.01–0.1 nm^{-1}) allows investigation of nanostructures which are in the range of 60–600 nm, therefore, motions of pore walls probably caused either by external or internal tensions are likely to underline the slow dynamics observed by XPCS. As it is well known, the elastic properties of polymer aerogels arises from their crosslinked structure which, in turn, presents spatial and dynamical heterogeneities.[10] In this sense, the slower dynamics of NC aerogels, with nanoparticles embedded in the polymer matrix forming the walls surrounding the pores, may reflect the entropic penalty that the polymer matrix suffers as a consequence of the establishment of interactions with the nanoparticles which are not present in the case of the pristine aerogel. The establishment of interactions between the nanoparticles and the polymer matrix led to a reinforcement of the material as demonstrated through oscillatory rheological measurements done for swollen samples.[30] The differences in the dependence of β with q in between the three samples under study may be interpreted as due to underlying differences in their respective microrheological properties as a consequence of the content of iron oxide nanoparticles.

IV. CONCLUSIONS

In summary, XPCS was employed to directly quantify the slow dynamics of aerogels and nanocomposite aerogels. All the samples under investigation, xerogels, aerogels, and nanocomposite aerogels with iron oxide NPs, present hyperdiffusive dynamics. We propose that the dynamics arises from the porous structure and not from the presence of the nanoparticles as commonly found for polymer nanocomposites. Polymer aerogels nanocomposites present longer relaxation times reflecting the entropic penalty that the polymer matrix suffers as a consequence of the establishment of interactions with the nanoparticles.

ACKNOWLEDGMENTS

Portions of this research were carried out at the light source Petra III at DESY, a member of the Helmholtz Association (HGF). We would like to thank F. Westermeier for assistance in using beamline P10. Financial support from Fundación Domingo Martinez and L´Óreal-Unesco fellowship FWIS and of MEC (Grant Nos. MAT2012-33517, MAT2011-23455, and MAT2011-24797) is gratefully acknowledged. Rebeca Hernández thanks MEC for a Ramon y Cajal contract.

[1]O. Wichterle, *Encyclopedia of Polymer Science and Technology* (Interscience, New York, 1971), Vol. 15.
[2]N. Kato and S. H. Gehrke, Colloids Surf., B **38**, 191 (2004).
[3]T. Lane, J. L. Holloway, A. H. Milani, J. M. Saunders, A. J. Freemont, and B. R. Saunders, Soft Matter **9**, 7934 (2013).
[4]R. A. Quirk, R. M. France, K. M. Shakesheff, and S. M. Howdle, Curr. Opin. Solid State Mater. Sci. **8**, 313 (2004).
[5]M. V. Risbud, A. A. Hardikar, S. V. Bhat, and R. R. Bhonde, J. Controlled Release **68**, 23 (2000).
[6]A. C. Pierre and G. M. Pajonk, Chem. Rev. **102**, 4243 (2002).
[7]F. Quignard, R. Valentin, and F. Di Renzo, New J. Chem. **32**, 1300 (2008).
[8]J. J. Yeo, Z. S. Liu, and T. Y. Ng, Modell. Simul. Mater. Sci. Eng. **21**, 075004 (2013).
[9]D. L. Abernathy, G. Grubel, S. Brauer, I. McNulty, G. B. Stephenson, S. G. J. Mochrie, A. R. Sandy, N. Mulders, and M. Sutton, J. Synchrotron Radiat. **5**, 37 (1998).
[10]A. Madsen, R. L. Leheny, H. Guo, M. Sprung, and O. Czakkel, New J. Phys. **12**, 055001 (2010).
[11]J. S. Higgins and H. C. Benoit, *Polymers and Neutron Scattering* (Oxford Science Publications, New York, 1994).
[12]Y. Shinohara, H. Kishimoto, N. Yagi, and Y. Amemiya, Macromolecules **43**, 9480 (2010).
[13]R. A. Narayanan, P. Thiyagarajan, S. Lewis, A. Bansal, L. S. Schadler, and L. B. Lurio, Phys. Rev. Lett. **97**, 075505 (2006).
[14]P. Falus, M. A. Borthwick, and S. G. J. Mochrie, Phys. Rev. Lett. **94**, 016105 (2005).
[15]A. Duri, T. Autenrieth, L. M. Stadler, O. Leupold, Y. Chushkin, G. Grubel, and C. Gutt, Phys. Rev. Lett. **102**, 145701 (2009).
[16]L. Cipelletti, S. Manley, R. C. Ball, and D. A. Weitz, Phys. Rev. Lett. **84**, 2275 (2000).
[17]K. Laszlo, A. Fluerasu, A. Moussaid, and E. Geissler, Soft Matter **6**, 4335 (2010).
[18]O. Czakkel, B. Nagy, E. Geissler, and K. Laszlo, J. Chem. Phys. **136**, 234907 (2012).
[19]S. Streit, C. Gutt, V. Chamard, A. Robert, M. Sprung, H. Sternemann, and M. Tolan, Phys. Rev. Lett. **98**, 047801 (2007).
[20]S. L. Candelaria, R. Chen, Y.-H. Jeong, and G. Cao, Energy Environ. Sci. **5**, 5619 (2012).
[21]S.-L. Loo, A. G. Fane, T.-T. Lim, W. B. Krantz, Y.-N. Liang, X. Liu, and X. Hu, Environ. Sci. Technol. **47**, 9363 (2013).
[22]S. Zheng, T. Wang, D. Liu, X. Liu, C. Wang, and Z. Tong, Polymer **54**, 1846 (2013).
[23]P. Akcora, S. K. Kumar, J. Moll, S. Lewis, L. S. Schadler, Y. Li, B. C. Benicewicz, A. R. Sandy, S. Narayanan, J. Ilavsky, P. Thiyagarajan, R. H. Colby, and J. F. Douglas, Macromolecules **43**, 1003 (2010).
[24]H. Oh and P. F. Green, Nat. Mater. **8**, 139 (2009).
[25]Y. Shinohara, H. Kishimoto, T. Maejima, H. Nishikawa, N. Yagi, and Y. Amemiya, Soft Matter **8**, 3457 (2012).
[26]D. Fragiadakis, L. Bokobza, and P. Pissis, Polymer **52**, 3175 (2011).
[27]F. Ehrburger-Dolle, I. Morfin, F. Bley, F. Livet, G. Heinrich, S. Richter, L. Piché, and M. Sutton, Macromolecules **45**, 8691 (2012).
[28]Y. Shinohara, A. Watanabe, H. Kishimoto, and Y. Amemiya, J. Synchrotron Radiat. **20**, 801 (2013).
[29]R. Hernández and C. Mijangos, Macromol. Rapid Commun. **30**, 176 (2009).
[30]R. Hernandez, J. Sacristan, A. Nogales, M. Fernandez, T. A. Ezquerra, and C. Mijangos, Soft Matter **6**, 3910 (2010).
[31]D. Kim, S. Srivastava, S. Narayanan, and L. A. Archer, Soft Matter **8**, 10813 (2012).
[32]R. L. Leheny, Curr. Opin. Colloid Interface Sci. **17**, 3 (2012).
[33]D. Orsi, L. Cristofolini, G. Baldi, and A. Madsen, Phys. Rev. Lett. **108**, 105701 (2012).
[34]H. Guo, G. Bourret, M. K. Corbierre, S. Rucareanu, R. B. Lennox, K. Laaziri, L. Piche, M. Sutton, J. L. Harden, and R. L. Leheny, Phys. Rev. Lett. **102**, 075702 (2009).
[35]A. Fluerasu, A. Moussaïd, A. Madsen, and A. Schofield, Phys. Rev. E **76**, 010401 (2007).
[36]M. Sutton, K. Laaziri, F. Livet, and F. Bley, Opt. Express **11**, 2268 (2003).
[37]C. Caronna, Y. Chushkin, A. Madsen, and A. Cupane, Phys. Rev. Lett. **100**, 055702 (2008).
[38]J. T. Koberstein, B. Morra, and R. S. Stein, J. Appl. Crystallogr. **13**, 34 (1980).
[39]P. Dieudonné, A. H. Alaoui, P. Delord, and J. Phalippou, J. Non-Cryst. Solids **262**, 155 (2000).
[40]B. S. Hsiao, K. H. Gardner, D. Q. Wu, and B. Chu, Polymer **34**, 3996 (1993).
[41]S. Narayanan, D. R. Lee, A. Hagman, X. F. Li, and J. Wang, Phys. Rev. Lett. **98**, 185506 (2007).